8. LASER COOLING AND TRAPPING OF NEUTRAL ATOMS

Curtis C. Bradley and Randall G. Hulet

Department of Physics and Rice Quantum Institute
Rice University
Houston, Texas

8.1 Introduction

The first proposal for using lasers to deflect atomic beams was made in 1970 [1], followed in 1975 by the suggestion to use laser light to slow and cool atoms [2, 3]. By 1978 the first successful experimental demonstrations of these ideas were realized [4–6]. Since then, the field has advanced at a rapid pace. It is now possible to laser cool atoms to below 1 μK, to confine as many as 10^{10} atoms in traps with densities of greater than 10^{12} cm^{-3}, and to trap atoms for time periods of up to one hour. Laser cooling techniques are also used to produce slow, monoenergetic atomic beams and to brighten beams by cooling the transverse motion.

In recent years, these techniques have begun to emerge from the specialist's laboratory and are being used in a variety of applications, including cold-atom collisions, time and frequency standards, investigations of quantum degenerate atomic gases, precision measurements of fundamental constants, measurements of parity-violating interactions, and searches for time-reversal–violating permanent electric dipole moments. This chapter is written for those wishing to exploit the properties of laser-cooled atomic gases, but who are not yet expert in the field. We begin with a description of two-level Doppler cooling and sub-Doppler cooling. Techniques for both longitudinal slowing and transverse cooling of atomic beams are presented next. Three types of atom traps are discussed, including pure magnetic, magneto-optical, and dipole traps. The chapter concludes with a brief treatment of evaporative cooling, which has recently been used to attain nano-Kelvin temperatures. We have chosen to focus on a few techniques that we feel are, or will be, the most useful. By necessity, then, large areas of the field are neglected or only briefly mentioned. This chapter is not intended to be an exhaustive review, but rather an introduction to the techniques and their capabilities. We apologize in advance for the many references and contributions that are not included. There are several excellent reviews meant for nonspecialists [7–15], and several special journal issues [16, 17] devoted to laser cooling and trapping. Laser cooling and atom trapping involve many of the

methods discussed in other chapters of this volume. Relevant chapters are Atomic Beams, Ion Trapping, Laser Stabilization, Diode Lasers, and Frequency Shifting and Modulation.

8.2 Laser Cooling

8.2.1 Doppler Cooling

The basic idea of laser cooling is that the photons of a laser beam can impart momentum to atoms. The simplest laser cooling, "Doppler cooling," involves just two atomic states, a ground state $|g\rangle$ and an excited state $|e\rangle$, and a laser beam tuned to near the $|g\rangle \leftrightarrow |e\rangle$ resonance frequency. In reality, of course, there are no two-level atoms, but one can be approximated by using a σ^+ or σ^- circularly polarized laser beam tuned to a $J \leftrightarrow J + 1$ transition. In this case, the atoms are optically pumped into the $m_J = \pm J$ ground state sublevel and can only be excited to the $m_J = \pm(J + 1)$ excited state sublevel. By absorbing a photon, the atom acquires the photon momentum $\hbar k_L$, where k_L is the wave vector of the laser field. The atom can lose its excitation energy by spontaneous or stimulated emission of a photon. If it is stimulated by the laser beam which originally excited it, the radiated photon rejoins the laser field in the same mode, and there is no net momentum transfer. On the other hand, spontaneous emission may result in a net change of momentum. The change in momentum from spontaneous decay of a photon with wave vector k_s is $\hbar k_s$. But because spontaneous emission is a symmetric process, so that wave vectors k_s and $-k_s$ are equally probable, $\langle k_s \rangle = 0$ and there is no net change in momentum on average in spontaneous decay. So, the round-trip process of stimulated absorption from $|g\rangle$ to $|e\rangle$ followed by spontaneous decay back to $|g\rangle$ results in an average momentum change of $\Delta p = \hbar k_L$. The rate of spontaneous decay is given by the product of the probability of being in state $|e\rangle$, ρ_{ee}, and the decay rate of $|e\rangle$, γ. Therefore, the average force exerted by the laser beam on the atoms is

$$\langle F \rangle = \left\langle \frac{\Delta p}{\Delta t} \right\rangle = \hbar k_L \rho_{ee} \gamma. \tag{1}$$

Since $\rho_{ee} \leq \frac{1}{2}$ in steady state, $\langle F \rangle \leq \frac{1}{2}\hbar k_L \gamma$. The surprisingly large maximum acceleration is given by

$$a_{\text{Dop}} = \frac{\hbar k_L \gamma}{2m} \tag{2}$$

where m is the atomic mass. For example, for the lithium $2s$–$2p$ transition, $\lambda = 671$ nm and $\gamma = (27.1 \text{ ns})^{-1}$, giving $a_{\text{Dop}} = 1.6 \times 10^8$ cm/s^2.

Viscous damping of atomic motion can be provided by two or more lasers that intersect symmetrically to form what is often referred to as optical molasses [18, 19]. In molasses, the forces on atoms are directed along the propagation vectors of the laser beams. The ultimate kinetic temperature, T, where $k_B T = \langle p^2/2m \rangle$, is determined by a balance of the laser-induced cooling and momentum diffusion. For spontaneously emitted photons, $\langle \mathbf{k}_s \rangle = 0$ and $\langle \mathbf{k}_s^2 \rangle > 0$. Spontaneous emission, therefore gives momentum diffusion for which $\langle p^2/2m \rangle > 0$. This results in laser-cooled atoms undergoing a random walk, or diffusion, out of the molasses region. The diffusion time τ_D is proportional to $\langle r^2 \rangle$, where r is the displacement due to diffusion. For alkali-metal atoms, τ_D is approximately 4 seconds for $r = 1$ cm. For certain "misalignments" of the molasses laser beams, it has been observed that τ_D can actually be increased by more than an order of magnitude [20, 21]. The lower temperature limit of Doppler cooling, T_{Dop}, can be estimated from the uncertainty in energy of the spontaneously emitted photon, $\hbar\gamma$. Calculations show that the Doppler cooling limit is given by $k_B T_{Dop} = \frac{1}{2}\hbar\gamma$ [22], which for lithium is 140 µK.

8.2.2 Sub-Doppler Cooling

As early as 1988, temperatures less than T_{Dop} were measured in optical molasses [23]. It was soon realized that optical pumping between the degenerate ground-state sublevels due to polarization gradients of certain configurations of laser polarization vectors could occur on time scales much slower than γ^{-1} and produce temperatures lower than T_{Dop} [24, 25]. Temperatures equal to several times the "recoil temperature," T_R, were measured in molasses. The recoil limit is set by the energy an atom acquires by recoiling from spontaneous emission, so $k_B T_R = (\hbar k_L)^2/m$. For ^{7}Li, $T_R = 6$ µK, while for ^{133}Cs, $T_R = 200$ nK. Temperatures of several times T_R are readily achieved in an optical molasses, when ambient magnetic fields are minimized [19].

Other sub-Doppler cooling techniques have been demonstrated, but have not yet been used in applications. One such method is adiabatic cooling, where atoms confined to the nodes of an optical standing wave are cooled through an adiabatic reduction of the standing wave intensity [26]. This technique has recently been demonstrated in three dimensions [27]. A particularly interesting *subrecoil* technique is velocity-selective coherent population trapping, or VSCPT, in which atoms are optically pumped into a coupled atomic/momentum state that decouples from the laser field for momenta equal to $\pm\hbar k_L$ [28, 29]. This method has also recently been demonstrated in two and three dimensions [30, 31]. For this technique, the width of the resulting momentum distribution is limited only by the interaction time. A different method that produces subrecoil temperatures uses the narrow linewidth of stimulated Raman transitions to provide atoms with very small velocity spread [32–34].

8.3 Atomic Beam Cooling

8.3.1 Longitudinal Slowing

The most important consideration for slowing an atomic beam with laser radiation is that the effective detuning Δ of the slowing laser changes as the atoms decelerate. This can easily be seen from Eq. (1), with

$$\frac{\Omega_0^2}{2\Omega_0^2 + 4\Delta^2 +} \tag{3}$$

$\Omega_0 = -2(\langle g|\mathbf{d}|e\rangle \cdot \mathbf{E})/\hbar \equiv \gamma(I/I_S)^{1/2}$ is the "on-resonance" Rabi frequency, where $\mathbf{d}$ is the atom's electric dipole moment, $\mathbf{E}$ is the laser electric field, I is the laser intensity, and I_S is the saturation intensity. The effective detuning depends on the velocity $\mathbf{v}$ of the atom, the laser beam wave vector $\mathbf{k}$, and the detuning Δ_0 of the laser for an atom at rest. Explicitly, $\Delta = \Delta_0 - \mathbf{k}\cdot\mathbf{v}$, where $\Delta_0 = \omega_L - \omega_0$, $\hbar\,\omega_L$ is the energy of a laser photon, and $\hbar\omega_0$ is the energy difference between states $|e\rangle$ and $|g\rangle$. The atoms in the beam are slowed by a single laser beam directed against their motion, such that in the frame of the moving atoms the laser frequency appears higher (bluer) than in the lab frame. However, as the atoms scatter photons and slow down, their Doppler shift is reduced until they effectively shift out of resonance and stop decelerating. In order to slow atoms over a larger range of velocity, some compensation for this changing Doppler shift must be made. The two most effective methods for doing this are chirp slowing [6, 35] and Zeeman slowing [36, 37].

For chirp slowing, the laser frequency is linearly chirped in time, so that Δ remains constant as atoms undergo a constant deceleration, a. The frequency is then reset to its initial value and the chirp repeats, slowing a new bunch of atoms. Table I shows some of the quantities relevant to both chirp and Zeeman slowing, for the alkali-metal elements. The time required to stop an atom with initial velocity v_0 is $\Delta t = v_0/a$. The required length of travel is

TABLE I. Quantities Relevant to Chirp and Zeeman Slowing for Alkali-Metal Elements

	T_0(K)	v_M (10^4 cm/s)	Δv_D (GHz)	λ (nm)	m (amu)	τ (ns)	a_{Dop} (10^6 cm/s^2)	Δt (ms)	ΔL (cm)
Li	900	19	2.8	617		27.1	160	1.2	115
Na	630	8.7	1.5	589	23	16.4	90	0.97	43
K	545	6.2	0.81	766	39	26		2.4	76
Rb	500	4.1	0.52	780	85	27		3.6	74
Cs	480	3.2	0.37	852	133	30.4	5.8	5.5	87

$$\Delta L = v_0 \Delta t - \frac{1}{2} a (\Delta t)^2 = \frac{v_0^2}{2a}. \tag{4}$$

From Chapter 1 (Eq. 1.32), the median velocity of an atom in the beam is

$$v_m = 1.30 \sqrt{\frac{2k_B T_0}{m}}, \tag{5}$$

where T_0 is the temperature of the atomic beam oven. The values of Δt and ΔL given in Table I assume $v_0 = v_m$ (T_0 selected for oven pressures of ~ 0.1 Torr) and $a = a_{Dop}$. The wavelength λ is for the principal $S_{1/2} \leftrightarrow P_{3/2}$ transition.

Two methods have been used to generate the required frequency chirp $\Delta v_D = v/\lambda$. A traveling-wave electro-optic modulator [35] can be used to produce frequency-modulated sidebands that can be swept in time, or the frequency of a laser diode may be ramped using the injection current [38]. Also, as an improvement over simple single-frequency chirp cooling, it is possible to use multiple laser frequencies in a relay-chirp cooling scheme [39, 40]. Still, there are two significant problems with the chirp slowing technique: (1) It may be technically difficult to sweep the frequency by the amount necessary to cool a significant portion of the velocity distribution, and (2) the atoms do not all arrive at their final velocity at the same longitudinal location. This, combined with the transverse spreading of the slowed atom beam, results in a significantly lower intensity of slow atoms than can be obtained with Zeeman slowing.

Zeeman slowing is, in several respects, a more powerful technique. Instead of the laser frequency being varied, the atoms' transition frequency is changed using a spatially varying magnetic field. For slowing to a specific final velocity, it is best to use the σ^- Zeeman slower design [41]. This type of Zeeman slower has its maximum magnetic field with an abrupt field cutoff at the downstream end, so the decelerating atoms are suddenly shifted out of resonance with the counterpropagating laser beam. This results in a minimal spread of slow atom velocities. For such a slower, the desired variation in the magnetic field is given by $\Delta B(z) \sim 1 - (1 - z/z_0)^{1/2}$, where z is the axial displacement along the slower, z_0 is given by $v_0^2/2a$, v_0 is the initial velocity of the fastest atoms to be slowed and a is the deceleration during slowing ($a > 0$). A solenoid having a current density $i(z) \sim i_0[1 - (1 - z/z_0)^{1/4}]$ produces an axial magnetic field with the correct spatial distribution. With this current distribution in mind, a fair approximation (see Fig. 1) of the ideal field is easily generated via stepped layers of windings around the tube of a vacuum nipple [42]. A double-stage Zeeman slower approach, in which the field decreases from a maximum and then rises again, allows slowing from higher initial velocities without resorting to larger solenoid current densities [43].

For either beam slowing technique, it is helpful to note that obtaining maximum slow atom flux does not necessarily require heroic efforts to slow the
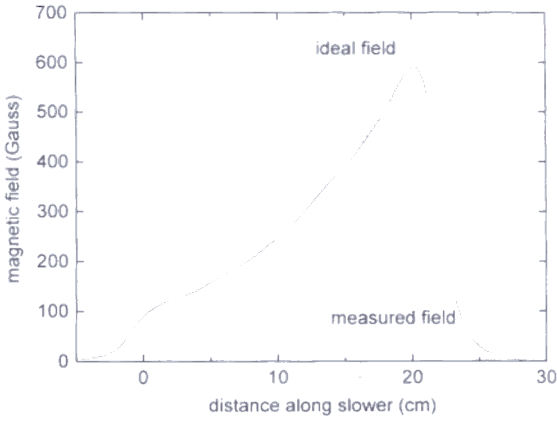
FIG. 1. Comparison of the ideal σ^- Zeeman slower magnetic field, designed for decelerating atoms at half the Doppler acceleration, with the measured values for a Zeeman slower used in our laboratory. Atoms with longitudinal velocities near 560 m/s begin to slow at ~0 cm along the slower. The rising magnetic field compensates for the decreasing Doppler shift of the decelerating atoms. The sharp cutoff of magnetic field just beyond ~20 cm helps to minimize the final longitudinal velocity spread of the Zeeman-slowed atoms.

entire thermal velocity distribution. Assuming a conventional atom beam source with the atom-slowing laser beam focused near the beam source aperture, is there an optimal choice of slower length which maximizes the slow atom production? As discussed previously, for a maximum initial velocity v_0 to be slowed, the slower length ΔL scales like v_0^2. Consequently, the useful atomic beam solid angle (set by the useable slow-atom–beam diameter) scales as $(\Delta L)^{-2} \sim v_0^{-4}$ (assuming deceleration starts immediately after the source). Since the integrated number of atoms to be slowed from a thermal beam only increases as v_0^4 or worse, the resultant flux of slow atoms is roughly independent of v_0, or equivalently, the slower length. This line of reasoning shows that a trap can be efficiently loaded directly from the slow atoms already present in a thermal atomic beam, if it is located close to the oven nozzle. Recently, magneto-optical traps have been loaded in this manner, with a small beam block in front of the trapped atoms to prevent trap loss via collisions with the atomic beam [44] . However, when beam slowing is required, a compact design, which is technically easier to build, may work as well as, or even better than, a slower designed to slow a large fraction of the thermal beam. For example, the σ^- Zeeman slower illustrated in Fig. 1 is designed to decelerate the slowest 1% of a thermal Li atom beam ($v_0 \leq 560$ m/s), using $a = a_{\text{Dop}}/2$. The slower solenoid produces a 100 G bias along its ~20 cm length and has a field maximum of 590 G. The solenoid consists of several layers

of heavily lacquered magnet wire wrapped around a double-wall vacuum nipple. It is energized by three separate current sources (allowing higher currents where needed, without the additional bulk of extra windings so it remains compact) and cooled externally with a fan and "internally" by circulating chilled water (passing inside the nipple's double wall) [42]. On a separate experiment we have installed a ~10 cm long σ^+ Zeeman slower which we use to load a Li magneto-optic trap. This slower was conceived and constructed in a couple of days, uses a single 1-amp current source, and is simply air-cooled.

8.3.2 Transverse Cooling and Beam Deflection

For many experiments it is necessary to increase the brightness of the slowed atomic beam. The simplest means of doing this is through a reduction of the beam divergence following longitudinal slowing. A 2-D molasses in a plane perpendicular to the atomic beam can significantly reduce the spread of transverse velocities of the slow atoms, such that the beam is effectively collimated.

For loading an atom trap, it is often desirable to separate the slow atoms from the residual fast atomic beam. Directing only the slow atoms toward the trap reduces trap loss caused by collisions with fast atoms. Furthermore, it is helpful to avoid the interaction between the longitudinal slowing laser beam and the trapped atoms. A simple means of doing this is to place the trap just off the atomic beam axis, behind a plate which blocks the fast atomic beam. As mentioned earlier, this approach can be used to effectively load a trap from an unslowed atomic beam [44]. Alternatively, a single laser beam directed transversely to the atom beam axis will deflect the slow atoms. For more precise control and larger angular deflection, the transverse laser beam can be cylindrically focused in the plane of the deflection with the slow atom fraction entering and leaving the laser beam along trajectories approximately perpendicular to the leading and trailing laser beam edges [1, 45]. Using this kind of slow atom beam deflection, alkali atoms with velocities of up to ~10^2 m/s can easily be deflected through angles of 30° or more. Several groups have also demonstrated methods for collimating and compressing slow atomic beams using laser light combined with inhomogeneous magnetic fields to provide exceptional slow atom beam brightening [46–48]. These brighteners are essentially two-dimensional versions of the magneto-optical trap described later.

8.4 Trapping

8.4.1 Magnetic Trapping

The first successful neutral atom trap was the quadrupole magnetic trap [49]. Any atom with a magnetic dipole moment μ will experience a force when located in a gradient of magnetic field. Atoms with their dipole moment aligned with the
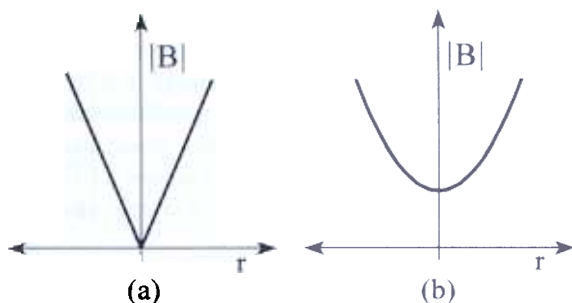
(a)   (b)

Fig. 2. Contrasting the two magnetic trap configurations. The spatial dependence of field strength is shown for (a) the quadrupole trap and (b) the Ioffe trap. For atoms with a linear Zeeman shift, such as the alkali metals, the trapping potential is proportional to the magnetic field strength $|\mathbf{B}|$.

field direction are attracted to a minimum of the field strength, while those antialigned are repelled. Three-dimensional local minima are easily produced with electromagnets or permanent magnets. Static local field maxima are ruled out by Earnshaw's theorem [50]. The most common magnetic trap configurations are the quadrupole trap and the Ioffe trap [51–53]. Comparing the two types (Fig. 2), the quadrupole trap has a linearly varying field which is more strongly confining than the quadradically varying field of the Ioffe trap, but exhibits a problematic zero-field point at its center. The Ioffe trap offers confinement with a nonzero field minimum.

A quadrupole field results, for example, from two current loops placed in an anti-Helmholtz orientation. For this configuration, the field is zero at a point between the current loops where the field components from each loop (and from other stray fields) exactly cancel. The on-axis field gradient near the trap minimum is given by $1.2 \pi NIDR^2(D^2 + R^2)^{-5/2}$ G cm/A, where R is the coil radius, $2D$ is the coil separation, and NI is the total current in each coil [54]. Axial and radial trap depth can be approximately equal for a coil separation of ~1.25 the coil radii, and for this case the gradient is given approximately by NIR^{-2} G cm/A. For 5 cm diameter coils carrying 10^3 amp-turns of current, the trap magnet field gradients are 160 G/cm, giving a trap depth of 11 mK/cm. Atoms remain confined because as they move about in the trap they adiabatically follow the changing field direction and stay in the same field-repelled spin state (as referred to the quantization direction given by the local magnetic field). Atoms that pass too close to the field zero, however, may undergo a nonadiabatic spin-flip or Majorana transition to the untrapped spin state because of the sudden change in field direction at the trap minimum [49]. The region very near the field zero, then, can act as a sinkhole for trapped atoms, becoming an important loss mechanism for atoms cooled to low kinetic temperatures. Fortunately, several

methods have been developed for effectively plugging the hole. One method is to introduce a weak, rotating, transverse magnetic field and thereby dynamically move the hole around in such a way as to prevent the atoms from falling into it (the TOP trap) [55]. A second approach is to repel the trapped atoms from the hole, via the optical dipole force from a blue-detuned laser beam focused on the trapping field minimum [56]. Typically, atoms are loaded into these traps by energizing the trapping coils and forming the trap around a cloud of atoms previously collected and laser-cooled by a combination of techniques including magneto-optic trapping and sub-Doppler molasses cooling. Using these methods, clouds of alkali atoms have been trapped with temperatures ranging from $\sim 20\,\mu K$ to ~ 1 mK and densities up to $\sim 10^{12}$ cm^{-3} [57].

A magnetic trap using a field in the Ioffe configuration provides a nonzero field minimum at the bottom of a harmonic potential. Because of the bias field there is no hole at the bottom. Also, because of the bias field, atoms in the trap can resonantly scatter many photons without being optically pumped to a nontrapped state. This allows for laser Doppler cooling of the atoms in the trap—a means for continuous loading of atoms from an atomic beam or vapor cell. Traps using this field configuration have been produced using conventional current distributions, superconducting coils, and permanent magnets. In our lab, more than 10^8 Li atoms have been confined and laser-cooled to $\sim 200\,\mu K$ in a trap made of six axially magnetized, cylindrical, high-flux NdFeB permanent magnets, positioned and aligned along three mutually orthogonal axes [58], as shown in Fig. 3. Near the center of the trap, the potential experienced by the atoms is harmonic with an oscillation frequency of $\sim 10^2$ Hz. The use of permanent magnets in building atom traps is motivated by the large field gradients that they offer [59, 60] and the desire to have good optical access to the trapped atoms along with overall experimental simplicity.

8.4.2 Magneto-Optic Trapping

A very robust trap, first demonstrated in 1987, uses the large dissipative force available from near-resonant laser light, in combination with an inhomogeneous magnetic field, to provide both spatial confinement and damping of atomic motion [61]. The most common configuration for such a magneto-optic trap (MOT) uses three mutually orthogonal pairs of counter propagating laser beams intersecting at the center of a quadrupole magnetic field, with polarizations set as shown in Fig. 4. An alternative arrangement for the laser beams uses a tetrahedral configuration of four beams [62]. In both versions, typical field gradient maxima are near 5 to 20 G/cm, with the field provided by two current-carrying coils placed in an anti-Helmholz configuration. This field distribution produces Zeeman shifts that are proportional to atomic displacement from the trap center. The appropriately polarized trap laser beams, along with these atomic energy
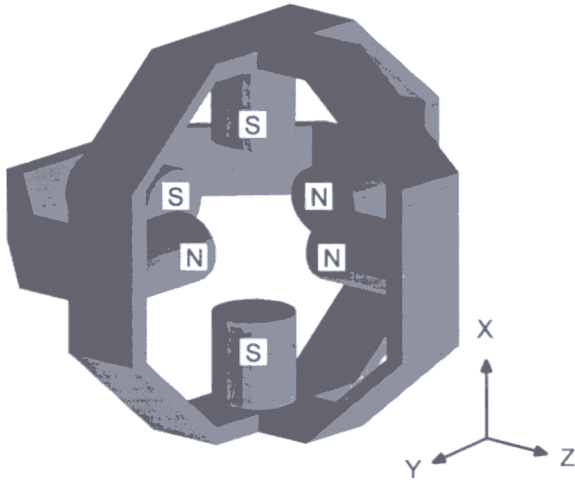
FIG. 3. Diagram showing the construction of our permanent magnet Ioffe trap. The six NdFeB cylindrical trap magnets are held by a magnetic-steel support, which also provides low reluctance paths for the flux to follow between magnets of opposite sign. The letters indicate the inner tip magnetizations of the magnets, N for north and S for south. The magnet tip-to-tip spacing is 4.45 cm.
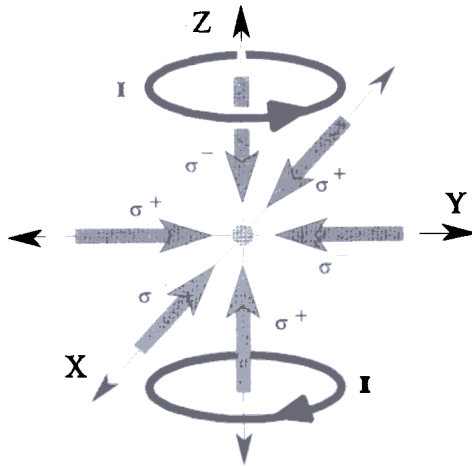

FIG. 4. The six-beam magneto-optic trap. Two coils, each carrying current I in the anti-Helmholtz configuration, provide a quadrupole magnetic field. At the magnetic field center, three pairs of opposing laser beams intersect to provide three-dimensional atom velocity damping. The arrangement of laser beam circular polarizations, given the current directions, are chosen in order to provide spatial confinement.

level shifts, provide a restoring force that keeps the atoms confined near the trap center. To see how this works, it is easiest to consider a simple atom with a $J = 0$, $m_J = 0$ ground state and a $J = 1$, $m_J = 0$, ± 1 excited state, with displacements along one trap axis, say the z-axis of Fig. 4. For atoms at positions $z \neq 0$, the $m_J = \pm 1$ excited states have opposite Zeeman shifts, as shown in Fig. 5. This asymmetry produces changes in the detunings for the $\sigma+$ and $\sigma-$ transitions (both are driven via the two opposing laser beams) that consequently lead to an imbalanced optical force for atoms at these positions. By properly arranging the laser polarizations relative to the magnetic field directions, the imbalanced optical forces can be directed inward toward the field center. Also, with the laser frequency detuned below the atomic resonant frequency, the atomic motion undergoes viscous damping. Using this type of trap, many groups have reported trapped atom clouds containing up to 10^8 atoms at temperatures of ~ 1 mK and below, with peak densities up to $\sim 10^{11}$ atoms/cm^{-3}. With careful balancing and alignment of the laser beams and control of the trap magnetic field, sub-Doppler cooling in a low-density MOT has been demonstrated, with observed
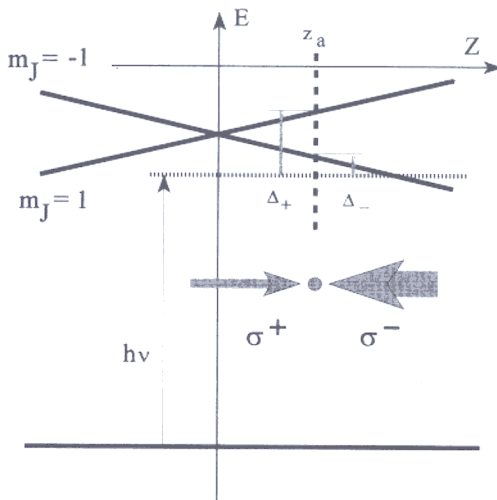

FIG. 5. Diagram showing origin of spatial confinement in magneto-optic traps. We consider a model atom with a $J = 0$ ($m_J = 0$) ground state and $J = 1$ excited state, situated at rest in a quadrupole magnet field, and interacting with opposing laser fields that drive $\Delta m_J = \pm 1$ transitions. The spatial dependence of the Zeeman-shifted levels results in a spatial dependence for the detunings of the two possible transitions. This asymmetry produces an imbalanced optical force that varies with the atom's position. For example, for an atom at $z = z_a > 0$ with the laser frequency v and polarizations as shown, the relative detunings, shown by $\Delta_\pm$, will cause the scattering rate for the σ^- transition to be relatively larger, and so the atom will be accelerated toward $z = 0$.

temperatures for trapped Cs as low as 10 μK [63–65]. Furthermore, by blocking the central portion of the hyperfine-repumping light, the central trapped atoms can optically pump into a hyperfine level which is only weakly coupled to the remaining laser beam light. This reduces the trap-losses caused by light scattering and results in increased trap densities. In such a *dark* spontaneous-force optical trap (Dark SPOT), densities of $\sim 10^{12}$ cm^{-3} have been reported [66].

8.4.3 Dipole-Force Trapping

The third type of trap utilizes the interaction of the induced atomic electric dipole moment with a gradient in an optical electric field. This type of trap is often referred to as a dipole-force trap. The light force potential for a two-level atom interacting with a sufficiently detuned and/or low-intensity light field is given by [67, 68]

$$U(\mathbf{r}) = \frac{\hbar \gamma^2}{8\Delta} \frac{I(\mathbf{r})}{I_S},$$

where I_s is the intensity required to saturate the two-level atom. Atoms can be confined at a maximum of $I(\mathbf{r})$, as at the focus of a laser beam, with Δ sufficiently large and negative. The first experimental demonstration of such a trap was in 1986 using Na atoms and a single ~ 200 mW laser beam, focused to a 10 μm spot, with the laser frequency tuned to ~ 0.6 THz below the D2 resonance frequency of sodium [69]. More recently, Rb has been trapped using a focused laser, detuned up to $\sim 10^2$ nm below the Rb D1 resonance [70]. There are several comparative disadvantages for this type of trap. The numbers of trapped atoms obtained to date are relatively small, typically $\sim 10^3$, largely because of the extremely small trapping volume. Also, because of the heating from scattered light, the lifetime of atoms in pure dipole-force traps is only ~ 0.2 seconds.

8.5 Evaporative Cooling

While there does not appear to be an ultimate laser cooling limit for a dilute atomic gas, at modest densities the poor optical transmission of the gas sample starts to interfere with the cooling mechanisms discussed. For alkali gases confined to a ~ 1 mm region, the on-resonance optical density becomes significant when the average atom density is only $\sim 10^{10}$ cm^{-3}. In order to further reduce the temperature of a sample of trapped atoms, while maintaining or increasing its density, a nonlaser technique is needed. Such a technique, evaporative cooling, was first proposed by Hess in 1986 [71] and demonstrated with magnetically trapped atomic hydrogen in 1988 [72], and has since been heavily relied upon to reach beyond laser cooling. By removing the most energetic fraction of the trapped gas and allowing sufficient time for rethermalization of

the remaining atoms via elastic collisions, it is possible to achieve dramatic cooling and compression of the gas. The initial method of doing this was to alter the trapping potential in order to provide a sufficiently low barrier. A more effective technique was suggested [8] in 1989 and successfully demonstrated in 1994 in magnetically trapped Na [73] and Rb [74]. In this newer version, atoms are "evaporated" via a forced spin-flip and their subsequent repulsion from the trapping region. In a magnetic trap, the most energetic atoms sample the largest magnetic fields and thereby experience the largest Zeeman shifts. By tuning an RF field to be resonant with atoms at relatively large fields, it is possible to remove a specific high-energy portion of the trapped atoms and leave the low-energy portion intact. After the remaining atoms rethermalize to a lower temperature, the RF frequency can be decreased and the process repeated [75]. Evaporative loss of trapped atoms competes with a separate trap-loss rate, typically from collisions with background gas particles, characterized by τ_{TRAP}. Because of this competition, it is necessary that the rethermalization via elastic collisions be sufficiently rapid for evaporative cooling to dominate and for significant increases in phase-space density to be obtained. An estimate of the average elastic collision rate is given by $R_E = n\sigma_E v$, where n is the average density, σ_E is the collisional cross section, and v is the average atom velocity in the trap. For successful evaporation, $R_E > 100/\tau_{TRAP}$ is required [76]. We take as an example evaporative cooling of Li vapor confined in a permanent magnet Ioffe trap. Given the measured triplet elastic cross-section for ^{7}Li atoms [77] of 5.0×10^{-13} cm^{-2} and an initial density of $\sim 10^{10}$ Li atoms/cm^3 at $\sim 200\ \mu$K, for successful evaporation the required τ_{TRAP} is ~ 400 seconds. We obtained this trapped atom lifetime by placing our trap inside a scrupulously cleaned ion-pumped chamber, by sourcing the trap through a small-diameter tube, and by evaporating titanium onto the inside of the ion-pump and trapping-chamber walls. The estimated background gas pressure is 10^{-12} torr.

Through the use of evaporative cooling of atoms in a trap, it is possible to increase the phase-space density (given by $d^3r\,d^3p$) of the trapped gas by many orders of magnitude. In the experiments that allowed the first observation of Bose-Einstein condensation in alkali-metal gases [56, 78, 79], evaporative cooling was used to boost the phase-space density by factors of $\sim 10^6$ over what was achieved with laser cooling alone. This breakthrough and other perhaps unanticipated phenomena are now accessible through the use of laser and evaporative cooling, and through the exploitation of the various types of atom traps.

References

1. Ashkin, A. (1970). *Phys. Rev. Lett.* **25**, 1321.
2. Hansch, T. W., and Schawlow, A. L. (1975), *Opt. Comm.* **13**, 68.

3. Wineland, D. J., and Dehmelt, H. (1975). *Bull. Am. Phys. Soc.* **20**, 637.
4. Wineland, D. J., Drullinger, R. E., and Walls, F. L. (1978). *Phys. Rev. Lett.* **40**, 1639.
5. Neuhauser, W., Hohenstatt, M., Toschek, P., and Dehmelt, H. (1978). *Phys. Rev. Lett.* **41**, 233.
6. Balykin, V. I., Letokhov, V. S., and Mushin, V. I. (1979). *JETP Lett.* **29**, 560.
7. Wineland, D. J., and Itano, W. M. (1987). *Physics Today* **40**, 34.
8. Pritchard, D. E., Helmerson, K., and Martin, A. G. (1989), in *Atomic Physics 11* (S. Haroche, J. C. Gay, and G. Grynberg, eds.), World Scientific, Singapore.
9. Cohen-Tannoudji, C., and Phillips, W. D. (1990). *Physics Today* **43**, 33.
10. Chu, S. (1991). *Science* **253**, 861.
11. Foot, C. J. (1991). *Contemp. Phys.* **32**, 369.
12. Chu, S. (1992). *Sci. Am.* **266**, 70.
13. *Proceedings of the International School of Physics "Enrico Fermi," Course CXVIII, (Varenna 1991): Laser Manipulation of Atoms and Ions* (E. Arimondo, W. D. Phillips, and F. Strumia, eds.), North-Holland, Amsterdam, 1992.
14. Metcalf, H., and van der Straten, P. (1994). *Phys. Reports* **244**, 204.
15. Aspect, A., Kaiser, R, Vansteenkiste, N., and Westbrook, C. I. (1995). *Physica Scripta* **T58**, 69.
16. *J. Opt. Soc. Am. B* **6**, 2020 (1989).
17. *Laser Physics* **4**, 829 (1994).
18. Chu, S., Hollberg, L., Bjorkholm, J. E., Cable, A., and Ashkin, A. (1985). *Phys. Rev. Lett.* **55**, 48.
19. Lett, P. D., Phillips, W. D., Rolston, S. L., Tanner, C. E., Watts, R. N., and Westbrook, C. I. (1989). *J. Opt. Soc. Am. B* **6**, 2084.
20. Chu, S., Prentiss, M. G., Cable, A., and Bjorkholm, J. (1987), in *Laser Spectroscopy VII* (W. Pearson and S. Svanberg, eds.), Springer-Verlag, Berlin.
21. Bagnato, V. S., Bigelow, N. P., Surdutovich, G. I., and Zilio, S. C. (1994). *Opt. Lett.* **19**, 1568.
22. Wineland, D. J., and Itano, W. M. (1979). *Phys. Rev. A* **20**, 1521.
23. Lett, P. D., Watts, R. N., Westbrook, C. I., Phillips, W. D., Gould, P. L., and Metcalf, H. J. (1988). *Phys. Rev. Lett.* **61**, 169.
24. Dalibard, J., and Cohen-Tannoudji, C. (1989). *J. Opt. Soc. Am. B* **6**, 2023.
25. Ungar, P. J., Weiss, D. S., Riis, E., and Chu, S. (1989). *J. Opt. Soc. Am. B* **6**, 2058.
26. Chen, J., Story, J. G., Tollett, J. J., and Hulet, R. G. (1992). *Phys. Rev. Lett.* **69**, 1344.
27. Kastberg, A., Phillips, W. D., Rolston, S. L., Spreeuw, R. J. C., and Jessen, P. S. (1995). *Phys. Rev. Lett.* **74**, 1542; Anderson, B. P., Gustavson, T. L., and Kasevitch, M. A. (1994), postdeadline paper contributed to the Ninth International Quantum Electronics Conference, Anaheim, California.
28. Aspect, A., Arimondo, E., Kaiser, R., Vansteenkiste, N., and Cohen-Tannoudji, C. (1989). *J. Opt. Soc. Am. B* **6**, 2112.
29. Mauri, F., and Arimondo, E. (1991). *Europhys. Lett.* **16**, 717.
30. Lawall, J., Bardou, F., Saubamea, B., Shimizu, K., Leduc, M., Aspect, A., and Cohen-Tannoudji, C. (1994). *Phys. Rev. Lett.* **73**, 1915.
31. Lawall, J., Kulin, S., Saubamea, B., Bigelow, N., Leduc, M., and Cohen-Tannoudji, C. (1995), to be published in *Phys. Rev. Lett.*.
32. Kasevich, M., Weiss, D. S., Riis, E., Moler, K., Kasapi, S., and Chu, S. (1991). *Phys. Rev. Lett.* **66**, 2297.
33. Reichel, J., Morice, O., Tino, G. M., and Salomon, C. (1994). *Europhys. Lett.* **28**, 477.

34. Davidson, N., Lee, H. J., Kasevich, M., and Chu, S. (1994). *Phys. Rev. Lett.* **72**, 3158.
35. Ertmer, W., Blatt, R., Hall, J. L., and Zhu, M. (1985). *Phys. Rev. Lett.* **54**, 996.
36. Phillips, W. D., and Metcalf, H. (1982). *Phys. Rev. Lett.* **48**, 596.
37. Phillips, W. D., Prodan, J. V., and Metcalf, H. J. (1985). *J. Opt. Soc. Am. B* **2**, 1751.
38. Sesko, D., Fan, C. G., and Wieman, C. E. (1988). *J. Opt. Soc. Am. B* **5**, 1225.
39. Salomon, C., and Dalibard, J. (1988). *C.R. Acad. Sci. Paris Ser. II* **306** 1319.
40. Bradley, C. C., Story, J. G., Tollett, J. J., Chen, J., Ritchie, N. W. M., and Hulet, R. G. (1992). *Opt. Lett.* **17**, 349.
41. Barrett, T. E., Dapore-Schwartz, S. W., Ray, M. D., and Lafyatis, G. P. (1991). *Phys. Rev. Lett.* **67**, 3483.
42. Tollett, J. J. (1995). "A Permanent Magnet Trap for Cold Atoms," Ph.D. Thesis, Rice University.
43. Witte, A., Kisters, T., Riehle, F., and Helmcke, J. (1992). *J. Opt. Soc. Am. B* **9**, 1030.
44. Anderson, B. P., and Kasevich, M. A. (1994). *Phys. Rev. A* **50**, R3581.
45. Nellessen, J., Müller, J. H., Sengstock, K., and Ertmer, W. (1989). *J. Opt. Soc. Am. B* **6**, 2149.
46. Nellessen, J., Werner, J., and Ertmer, W. (1990). *Opt. Comm.* **78**, 300.
47. Riis, E., Weiss, D. S., Moler, K. A., and Chu, S. (1990). *Phys. Rev. Lett.* **64**, 1658.
48. Scholz, A., Christ, M., Doll, D., Ludwig, J., and Ertmer, W. (1994). *Opt. Comm.* **111**, 155.
49. Migdall, A. L., Prodan, J. V., Phillips, W. D., Bergeman, T. H., and Metcalf, H. J. (1985). *Phys. Rev. Lett.* **54**, 2596.
50. Wing, W. H. (1984). *Progress in Quantum Electronics* **8**, 181.
51. Gott, Y. V., Ioffe, M. S., and Tel'kovskii, V. G. (1962). *Nucl. Fusion 1962 Suppl.* **Pt. 3**, 1045.
52. Bagnato, V. S., Lafyatis, G. P., Martin, A. G., Raab, E. L., Ahmad-Bitar, R. N., and Pritchard, D. E. (1987). *Phys. Rev. Lett.* **58**, 2194.
53. Hess, H. F., Kochanski, G. P., Doyle, J. M., Masuhara, N., Kleppner, D., and Greytak, T. J. (1987). *Phys. Rev. Lett.* **59**, 672.
54. Bergeman, T., Erez, G., and Metcalf, H. J. (1987). *Phys. Rev. A* **35**, 1535.
55. Petrich, W., Anderson, M. H., Ensher, J., Cornell, R., and Cornell, E. A. (1995). *Phys. Rev. Lett.* **74**, 3352.
56. Davis, K. B., Mewes, M.-O., Andrews, M. R., van Druten, N. J., Durfee, D. S., Kurn, D. M., and Ketterle, W. (1995). *Phys. Rev. Lett.* **75**, 3969.
57. Davis, K. B., Mewes, M.-O., Joffe, M. A., Andrews, M. R., and Ketterle, W. (1995). *Phys. Rev. Lett.* **74**, 5202.
58. Tollett, J. J., Bradley, C. C., Sackett, C. A., and Hulet, R. G. (1995). *Phys. Rev. A* **51**, R22.
59. Tollett, J. J., Bradley, C. C., and Hulet, R. G. (1992). *Bull. Am. Phys. Soc.* **37**, 1126.
60. Frerichs, V., Kaenders, W. G., and Meschede, D. (1992). *Appl. Phys. A* **55**, 242.
61. Raab, E. L., Prentiss, M., Cable, A., Chu, S., and Pritchard, D. E. (1987). *Phys. Rev. Lett.* **59**, 2631.
62. Shimizu, F., Shimizu, K., and Takuma, H. (1991). *Opt. Lett.* **16**, 339.
63. Steane, A. M., Chowdhury, M., and Foot, C. J. (1992). *J. Opt. Soc. Am. B* **9**, 2142.
64. Cooper, C. J., Hillenbrand, G., Rink, J., Townsend, C. G., Zetie, K., and Foot, C. J. (1994). *Europhys. Lett.* **28**, 397.

65. Wallace, C. D., Dinneen, T. P., Tan, K. Y. N., Kumarakrishnan, A., Gould, P. L., and Javanainen, J. (1994). *J. Opt. Soc. Am. B* **11**, 703.
66. Ketterle, W., Davis, K. B., Joffe, M. A., Martin, A., and Pritchard, D. E. (1993). *Phys. Rev. Lett.* **70**, 2253.
67. Gordon, J. P., and Ashkin, A. (1980). *Phys. Rev. A* **21**, 1606.
68. Dalibard, J., and Cohen-Tannoudji, C. (1985). *J. Opt. Soc. Am. B* **2**, 1707.
69. Chu, S., Bjorkholm, J. E., Ashkin, A., and Cable, A. (1986). *Phys. Rev. Lett.* **57**, 314.
70. Miller, J. D., Cline, R. A., and Heinzen, D. J. (1993). *Phys. Rev. A* **47**, R4567.
71. Hess, H. F. (1986). *Phys. Rev. B* **34**, 3476.
72. Masuhara, N., Doyle, J. M., Sandberg, J. C., Kleppner, D., Greytak, T. J., Hess, H. F., and Kochanski, G. P. (1988). *Phys. Rev. Lett.* **61**, 935.
73. Davis, K. B., Mewes, M.-O., Joffe, M. A., and Ketterle, W., (1994), contributed paper to the Fourteenth International Conference on Atomic Physics, University of Colorado, Boulder, Colorado.
74. Petrich, W., Anderson, M. H., Ensher, J. R., and Cornell, E. A., (1994), contributed paper to the Fourteenth International Conference on Atomic Physics, University of Colorado, Boulder, Colorado.
75. Davis, K. B., Mewes, M.-O., and Ketterle, W. (1995). *Appl. Phys. B* **60**, 155.
76. Monroe, C. R., Cornell, E. A., Sackett, C. A., Myatt, C. J., and Wieman, C. E. (1993). *Phys. Rev. Lett.* **70**, 414.
77. Abraham, E. R. I., McAlexander, W. I., Sackett, C. A., and Hulet, R. G. (1995). *Phys. Rev. Lett.* **74**, 1315.
78. Anderson, M. H., Ensher, J. R., Matthews, M. R., Wieman, C. E., and Cornell, E. A. (1995). *Science* **269**, 198.
79. Bradley, C. C., Sackett, C. A., Tollett, J. J., and Hulet, R. G. (1995). *Phys. Rev. Lett.* **75**, 1687.